Journal of Molecular Liquids 377 (2023) 121576

Contents lists available at ScienceDirect

Journal of Molecular Liquids

journal homepage: www.elsevier.com/locate/molliq

PMMA nano-encapsulated phase change material colloids for heat management applications

Filippo Agresti [a,*], David Cabaleiro [b], Laura Fedele [c], Stefano Rossi [c], Simona Barison [a]

[a] CNR-ICMATE, Corso Stati Uniti 4, I-35127 Padova, Italy
[b] CINBIO, Dpto. Física Aplicada, Universidade de Vigo, E-36310 Vigo, Spain
[c] CNR-ITC, Corso Stati Uniti 4, I-35127 Padova, Italy

ARTICLE INFO

Article history:
Received 13 January 2023
Revised 23 February 2023
Accepted 2 March 2023
Available online 6 March 2023

Keywords:
Nano-encapsulation
PCM
Emulsion polymerization
PMMA

ABSTRACT

Phase Change Materials (PCM) emulsions or micro-nano-encapsulated into organic and inorganic shells have attracted scientific interest for their potential to enhance the thermal capacity and the efficiency of heat transfer liquids. In this work, RT21HC, a commercial PCM with transition temperature at 21 °C, has been successfully nano-encapsulated into Poly(methyl-methacrylate) (PMMA) shells by an emulsion polymerization process after the selection of proper surfactant and synthesis parameters, in order to obtain complete encapsulation and stable colloidal dispersions. Water-based colloidal dispersions containing 10 wt% PCM were obtained and characterized from point of view of microstructure, colloidal stability, rheological properties, apparent heat capacity and thermal diffusivity, in order to show the potential of these colloidal dispersions as advanced heat management fluids. With the aim to mitigate the phenomenon of PCM crystallization supercooling that is caused by nano-confinement and is cause of apparent thermal capacity loss, the effect of incorporation into the nano-capsules of two fatty esters, two fatty alcohols and a fatty acid as nucleating agents, has also been studied.

1. Introduction

Achieving higher levels of energy efficiency represents one of the main challenges and targets for the near future by various international institutions and for humanity in general, in order to mitigate the precariousness in the supply of some energy resources, as recently experienced due to the war in Ukraine, and to address the need to deal with the enormous issue of climate change caused by greenhouse gas emissions. EU has recently updated its energy efficiency targets for 2030 as part of the European Green Deal package, with the objective to reduce greenhouse gas emissions of at least 55%, with a reduction of 36% for final energy consumption and 39% for primary energy consumption by 2030 compared to the 2007 Reference Scenario. The achievement of these ambitious and noble objectives also passes through the development of more efficient technologies in the field of heat storage and transfer, able to exploit renewables more effectively. Actually, heating and cooling constitutes about 50% of total EU energy consumption and, according the European Green Deal's Climate Target Plan, it is necessary to increase renewable energy shares in this sector in order to achieve the EU's energy and climate targets cost-effectively [1].

Phase change material emulsions (PCMEs) and nano-encapsulated PCMs have risen interest in recent years as potential heat transfer and heat storage fluids, capable of increasing the energy efficiency of facilities in which the fluids are used. These new materials consist of a base fluid, a suitable heat transfer fluid, and an emulsified or an encapsulated PCM, which should be immiscible with the base fluid [2–7]. The idea is to exploit the latent heat of melting and crystallization of PCM to increase the apparent thermal capacity of the system conferring increased thermal storage and transfer properties. The continuous phase, the base fluid, confers greater thermal conductivity and lower viscosity than PCM. The emulsified or encapsulated PCM have also the advantage to be pumped through a heat transfer circuit independently from the physical state of dispersed droplets/particles. One of the two main problems related to these systems is the phenomenon of supercooling, i.e. the reduction of the crystallization temperature caused by the fact that the process generally proceeds by homogeneous nucleation, and therefore through the formation and growth of nuclei, whose probability is greatly reduced in nanoconfined systems [8]. The second is the colloidal instability that is caused by different phenomena, such as coalescence of emulsion droplets that causes their aggregation and growth, Ost-

* Corresponding author.
E-mail address: filippo.agresti@cnr.it (F. Agresti).

https://doi.org/10.1016/j.molliq.2023.121576
0167-7322/

wald ripening that is a thermodynamically driven process causing the growth of big droplets at the expenses of smaller ones and phase inversion/phase separation due to temperature or composition changes. Colloidal instability can cause phase separation and creaming phenomena that hinder the functional properties of the PCM emulsion system. One of the strategies to improve colloidal stability and PCM coalescence and leakage is micro-encapsulation (capsules with sizes in the 1 μm to 1000 μm range) and nano-encapsulation (1–1000 nm range) into solid and stable shells. Mainly organic shells have been considered for these applications such as formaldehyde derivatives, PMMA, polystyrene, Arabic gum, chitosan/gelatin, amino plastics, agar/gelatin/gum Arabic, urea–formaldehyde resin, to cite some. Several physical (spray drying and cooling, vibrational nozzle, centrifugal extrusion, solvent evaporation etc.) and chemical methods that are mainly polymerization methods, have been developed so far [9].

The micro and nano-encapsulation of organic PCMs into PMMA shells has already been reported by different authors, with particular interest towards the study of the physico-chemical properties of the capsule/PCM system [10–14] for thermal energy storage applications, but more rarely towards the properties of colloidal suspensions of them [15,16], that could serve as advanced heat management fluids.

In this work, a commercial PCM material, RT21HC, with nominal phase change temperature at 21 °C, has been successfully nano-encapsulated into Poly(methyl-methacrylate) (PMMA) through a one-pot emulsion polymerization method. Stable, concentrated colloidal suspensions of the nano-capsules in water have been produced with the aim of studying their performances as heat transfer and heat storage fluids. We also show that by incorporating five different organic nucleating agents (two fatty esters, two fatty alcohols and a fatty acid) into the nano-capsules it is possible to mitigate the phenomenon of supercooling that affects nano-confined systems.

2. Materials and methods

In the synthesis of each of the 6 PMMA-nanoencapsulated PCM dispersions investigated in this work, three solutions have been prepared: solution A has been obtained by dissolving 0.037 g of Sodium-dodecylsulfate (SDS, greater than 99%, provided by Sigma-Aldrich) into deionised water (Millipore, Billerica MA, USA, 18.2 MΩ cm); solution B by mixing 3 g of RT21HC, a paraffin based material commercialised by Rubitherm Technologies GmbH as a PCM (nominal phase change temperature of 21 °C with heat storage capacity of 190 J/g including latent and sensible heat in the 13–28 °C temperature range), 6 g of methyl-methacrylate (MMA, 99 % provided by Alfa -Aesar) and in some cases 0.3 g of a nucleating agent reported later in this section; solution C by dissolving 0.04 g of ammonium peroxydisulfate (APS, 98% provided by Alfa-Aesar) into deionised water, used as MMA polymerization initiator. An intermediate emulsion has been obtained by slowly adding solution B to solution A at 25 °C under stirring and ultrasonication using a Sonics VCX-130 tip-sonicator operated at 50 W and 20 kHz for 5 min. Once the emulsion has been prepared, Solution C containing the polymerization initiator has been added and the temperature of the mixture has been raised to 85 °C for about 1 h, until the total weight reduced to 30 g by water evaporation. All the described operations have been carried out under pure nitrogen stream. The five nucleating agents that have been tested are PCM materials with transition temperatures in the range 30–60 °C and different chemical properties: two alcohols are 1-octadecanol (melting point (MP) = 59 °C) and 1-hexadecanol (MP = 46 °C); two esters are methyl-stearate (MP = 37–41 °C) and methyl-palmitate (MP = 32–35 °C); the fatty acid is dodecanoic acid (MP = 44 °C). Sample R is the reference sample, prepared without a nucleating agent; samples OD, HD, MS, MP and DA are those containing respectively 1-octadecanol, 1-hexadecanol, methyl-stearate, methyl-palmitate and dodecanoic acid as nucleating agents. The final concentration of PCM into the colloids is 10 wt% and that of nucleating agent is 1 wt%, where present. Table 1 reports a summary on samples compositions and main data on PCM and nucleating agents.

A Malvern Zetasizer Nano ZS based on dynamic light scattering (DLS) technique has been used for the evaluation of particles size distribution within the colloids and ζ-potential. Thermal diffusivity measurements with statistical uncertainty of 2% were carried out in the 14–32 °C temperature range using a home-made device exploiting the photoacoustic effect. Details about the technique and device are reported elsewhere [17]. The solid–liquid transitions of encapsulated PCM have been investigated using a differential scanning calorimeter DSC Q2000 (TA Instruments), equipped with a refrigerated cooling system RCS 90. Experiments were performed at scanning rates of 1–5 °C/min, in hermetically-sealed aluminum T_{zero} pans and under inert N_2 atmosphere. Dynamic viscosities (μ) have been obtained utilizing a rotational rheometer Physica MR-101 (Anton Paar) operating with a coaxial-cylinder geometry (cup: CC27/T200/SS and bob: B-CC27/P6) and a Peltier jacket P-PTD 200. Flow curves were obtained at temperatures ranging from 10 to 50 °C and shear rates between 1 and 100 s^{-1}. The residual powders deriving from dried colloids have been observed via field-emission scanning electron microscopy (FE-SEM) with a SIGMA Zeiss instrument (Zeiss Microscopy GmbH Germany), operating in high-vacuum conditions at an accelerating voltage of 20 kV. Sample R and its residual solid have been investigated by X-ray diffraction using a Malvern-Panalytical Empyrean diffractometer using the Cu-K_α radiation and a PIXcel3D solid state detector.

3. Discussion

All the samples obtained with the procedure described in the previous section look as white stable colloidal dispersions. Fig. 1 shows a diagram representing samples preparation procedure and a picture of sample R that is representative of all samples.

The procedure exploits an emulsion polymerization process to create colloidal dispersions of capsules of PMMA containing RT21HC PCM in water. The initial emulsion is made up of droplets containing the MMA monomer and PCM, where, due to the slight solubility of MMA in water, a gradient with a higher concentration towards the droplet/water interphase is established, while RT21HC is virtually insoluble in water. The higher concentration of MMA at the interphase allows its interaction with APS initiator, which is injected into the continuous phase, whose dianion dissociates to give radicals according to the equilibrium:

$$[O_3SO{-}OSO_3]^{2-} \rightleftharpoons 2\ [SO_4]^{\cdot -}$$

that catalyse the polymerization reaction of MMA at 85 °C to give the formation of PMMA capsules.

In order to investigate the nature of the dispersed material that has been obtained through the emulsion polymerization procedure, drops of diluted samples have been dried on aluminium sample holders and observed by FE-SEM. Fig. 2 shows micrographs of all resulting solids.

The micrographs show the actual formation of PMMA capsules in all samples with sizes in the 25–80 nm and similar morphologies. The capsules appear almost spherical with sometimes polyhedral deformations that are probably due to the packing during the drying process and the high concentration. Where the packing of particles is lower, as shown for sample MP, the appearance is more

Table 1
Samples composition summary.

Sample name	PCM				Nucleating Agent (NA)		
	Commercial name	Melting T (°C)	Latent Heat (kJ/kg)	Concentration into final colloid	Chemical name	Melting T (°C)	Concentration into final colloid
R	RT21HC	21 °C	190	10 wt%	Reference sample, no NA	–	1 wt%
OD					1-octadecanol	59	
HD					1-hexadecanol	46	
MS					methyl-stearate	37–41	
MP					methyl-palmitate	32–35	
DA					dodecanoic acid	44	

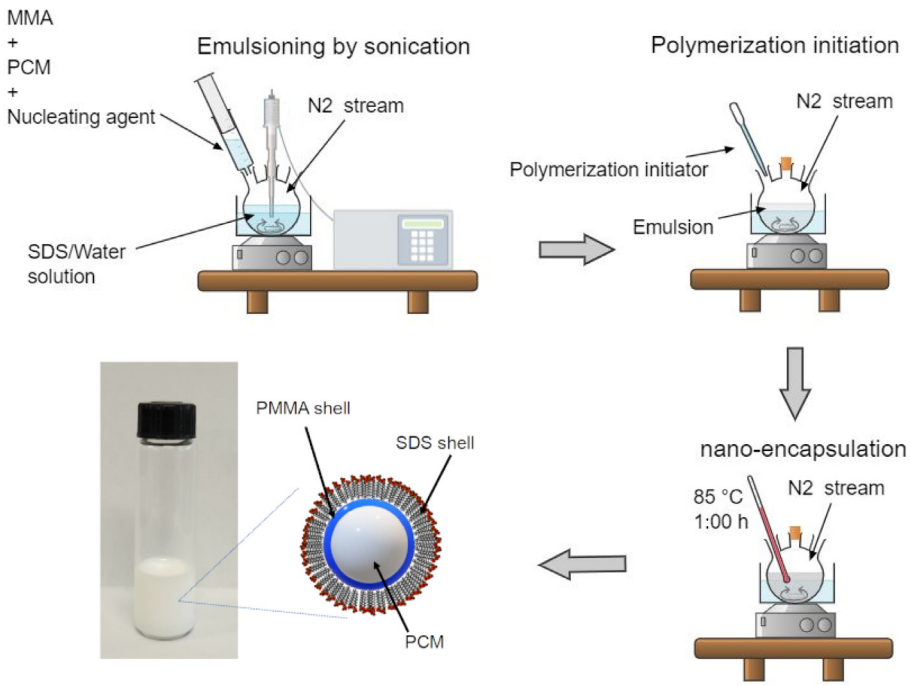

Fig. 1. Diagram showing the nano-encapsulated PCM colloids preparation.

spherical. In some cases, as shown for sample OD, sporadic exploded or incomplete capsules are also visible, showing the internal hollow structure.

Fig. 3a shows the XRD profiles of colloid R, above and below RT21HC melting point and that of corresponding residual dry solid. The XRD of colloid above melting temperature has broad bands due the contribution of PMMA around 14°, incapsulated liquid RT21HC at 20° and water at about 29° and 42°. Below the melting point of RT21HC two peaks at 21.5° and 23.5° appear, corresponding to its crystalline form, while the broad amorphous band at 20° disappears, corresponding to its liquid form. The same behavior is observed for the residual dry solid, where in absence of the contribution from water, the quasi-amorphous peaks of PMMA at 14°, 29° and 42° are discernible. The time resolved XRD in the 15°-30° range of colloid R during the heating from 10 °C to room temperature in Fig. 3b shows the detail of complete melting of the incapsulated RT21HC in about 15 min.

Table 2 shows a resume of colloidal properties obtained using a Malvern Zetasizer Nano ZS. All samples show high negative ζ-potentials due to the absorption of SDS on the surface of capsules, indicating good emulsion stability, though some degree of aggregation is present, considering the difference of Z-Ave values with respect to what is observed from SEM micrographs. With exception of sample MS, all other colloids containing a nucleating agent show higher Z-Ave values and Polydispersity Indexes with respect to sample R.

Fig. 4 shows thermal diffusivity measurements obtained with a photo-thermo-acoustic device, of the colloids, compared to that of water. The temperature region where phase change happens has been cut since it leads to meaningless artifacts on thermal diffusivity. All samples show lower thermal diffusivity values with respect to pure water of the order of 6–10% due to the lower diffusivity of dispersed materials (especially in solid state) compared to water.

Fig. 5 shows DSC profiles of all colloidal dispersions. The presence of nucleating agents does not seem to affect the melting process: the onset of the peak, that is at 18.5 °C for sample R, its shape and the area giving a latent heat of 11.9 J/g change only slightly by adding nucleating agents. Conversely, the onset of solidification peak is much more affected, since nucleation and subsequent growth of crystals is the process more kinetically hindered, espe-

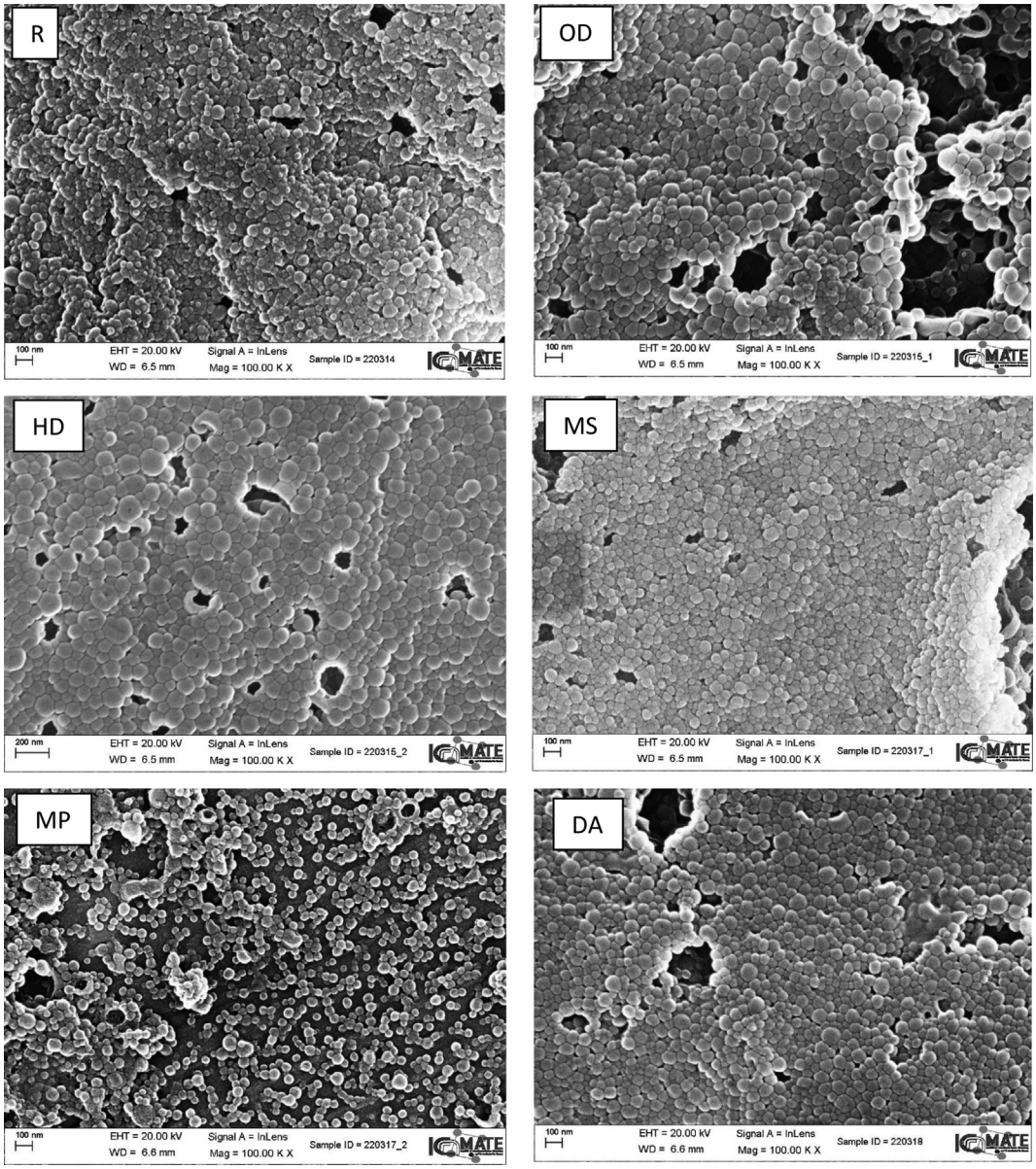

Fig. 2. FE-SEM of dried samples. Sample R (a); sample OD (b); sample HD (c); sample MS (d); sample MP (e); sample DA (f).

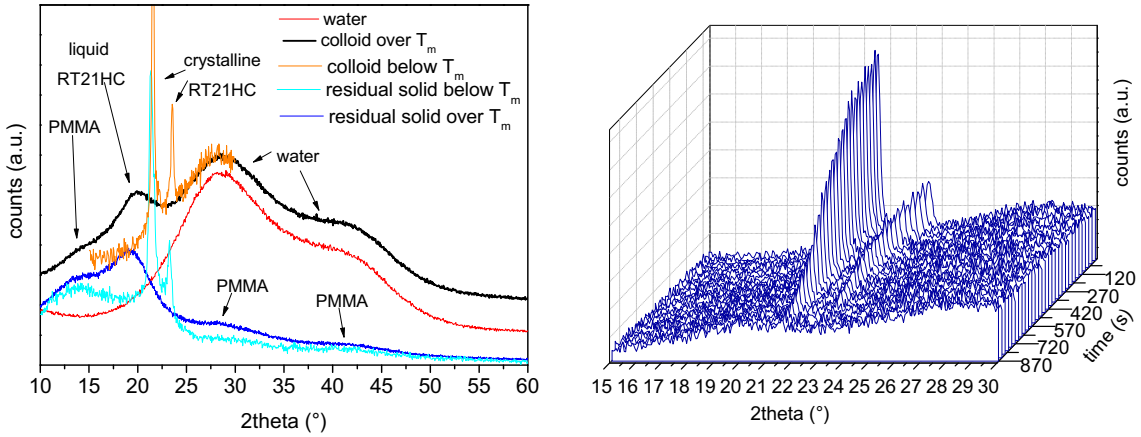

Fig. 3. (a) XRD profiles of colloid R and its residual solid above and below RT21HC melting temperature. (b) Time resolved XRD profiles of colloid R during RT21HC melting.

Table 2
DLS and ζ-potential results.

Sample	DLS Z-Ave (nm)	Polydispersity Index	ζ-potential (mV)
R	145	0.17	−70
OD	179	0.32	−55
HD	161	0.24	−83
MS	152	0.17	−82
MP	207	0.28	−83
DA	162	0.25	−77

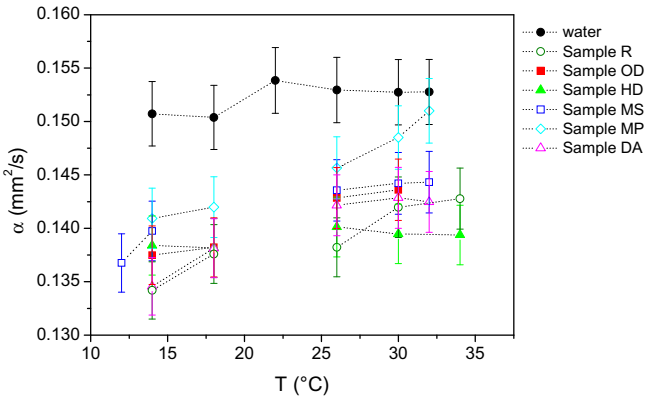

Fig. 4. Thermal diffusivity of colloids compared to water.

cially into nano-confined systems like this, because the probability of formation of a nucleus and its growth is proportional to the involved volume.

Crystallization onset is at about 10.7 °C for sample R. Sample OD shows the least supercooling with two main exothermic peaks, the first with onset already at about 19 °C and the second around 13 °C. Sample HD shows a similar behavior but with higher supercooling, with first peak at about 16.7 °C and second at 8.4 °C. Multiple endothermic contributions are also present for sample DA, even if not so broad, with first onset around 14–15 °C and second around 9 °C. Samples MP and MS, containing the two esters, show behaviors more similar to sample R with one single endothermic contribution with onset at 10.4 °C and 11.3 °C, respectively. Fig. 6 reports the apparent thermal capacity enhancement of each colloid with respect to pure water, considering these DSC data, calculated as:

$$\Delta H_{\%} = 100\left(\frac{\left(X_{PCM}c_{P_{PCM}} + X_{PMMA}c_{P_{PMMA}} + X_{water}c_{p_{water}}\right)\Delta T + L_{PCM}}{c_{p_{water}}\Delta T} - 1\right) \quad (1)$$

where X_{PCM}, X_{PMMA}, and X_{water} are the weight fractions of PCM, PMMA capsules and water, respectively; $c_{P_{PCM}}$, $c_{P_{PMMA}}$ and $c_{p_{water}}$ are the corresponding specific heats; L_{PCM} is the measured latent heat of phase change of encapsulated PCM; ΔT is the real working range evaluated from DSC measurements, as the temperature difference between the end-sets of melting and solidification processes. This

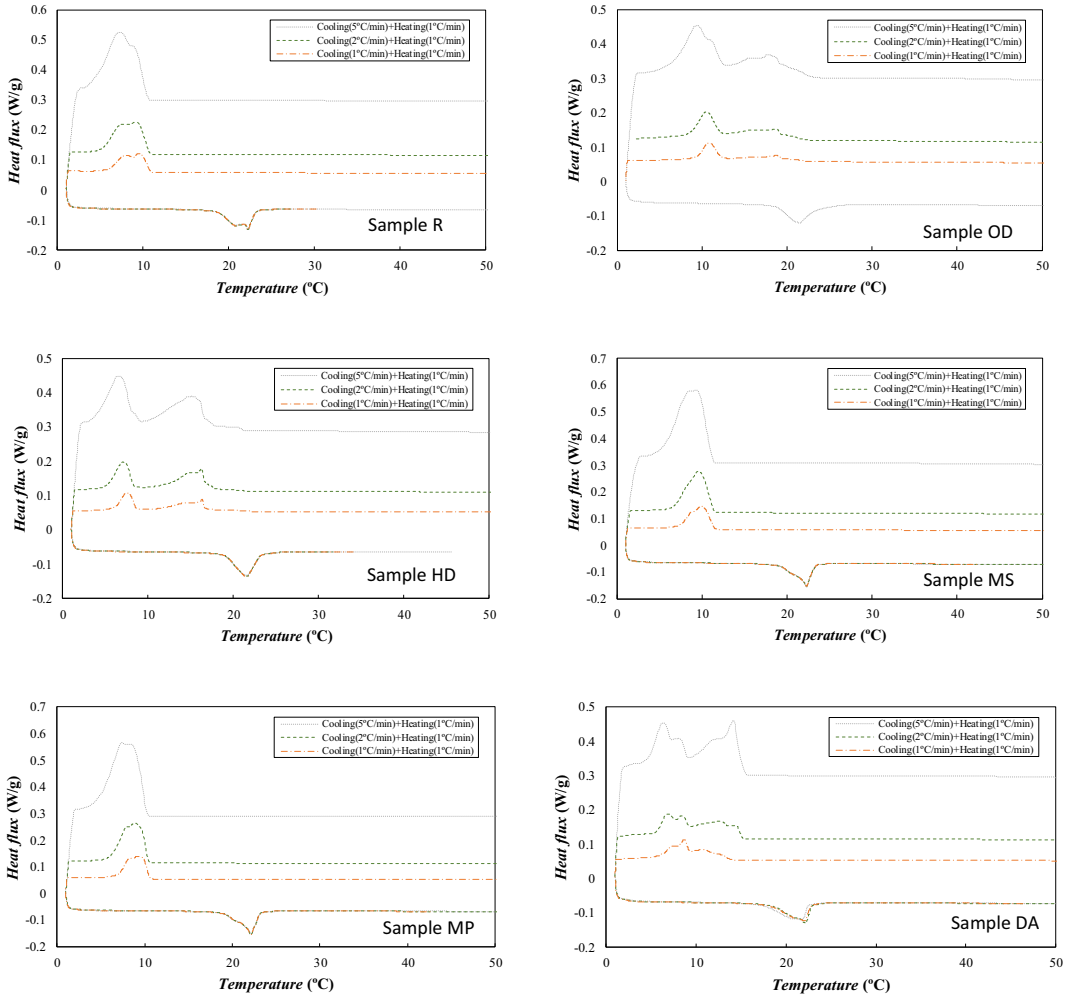

Fig. 5. DSC profiles of colloids at 1 °C/min heating rate and 1–5 °C/min cooling rate. Sample R (a); sample OD (b); sample HD (c); sample MS (d); sample MP (e); sample DA (f).

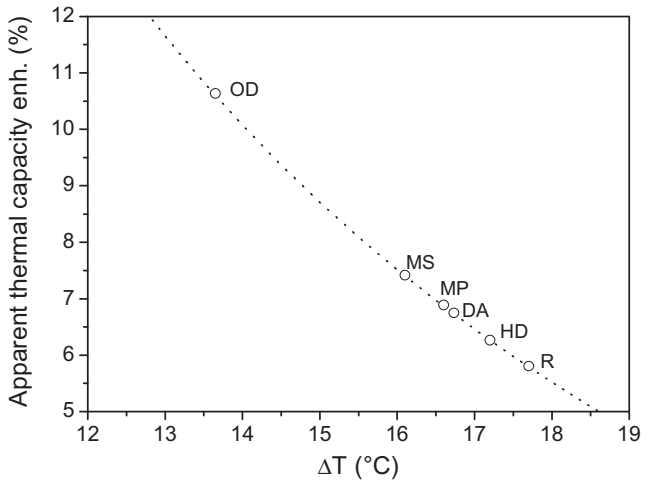

Fig. 6. Apparent thermal capacity enhancement as a function of least temperature working range, compared to pure water.

graph shows that OD resulted as the best nucleating agent, giving > 10% enhancement of emulsion thermal capacity within a ΔT of 14 °C. This enhancement is of course related to the working temperature range that is mainly determined by the supercooling. Hence, the mitigation of this phenomenon with effective nucleating agents is of paramount importance to shrink the temperature working range around the transition temperature and boost-up the apparent thermal capacity of these colloids.

Dynamic viscosity measurement for all samples collected at 10 °C and 40 °C, below and above the PCM melting temperature respectively, compared with water as a reference, are shown in Fig. 7. The viscosity of all colloids is of course increased with respect to water due to the presence of colloidal capsules with an average increase of about 130%, both at 10° and 40 °C, except for samples containing the two fatty alcohols as nucleating agents, i.e. samples OD and HD that also show a non-Newtonian shear-thinning behaviour that is more evident especially at lower temperature. The shear-thinning behaviour is often observed in concentrated colloidal systems and its origin has been matter of debate into the scientific community [18,19]. Fluid layering perpendicular to shear gradient has been pointed to as one of the possible origins of the phenomenon [20,21], while other authors pointed to the influence of particle stiffness on the appearance of the phenomenon [22], or to the decrease in the relative contribution of entropic forces during shear application [18]. In the case of present study, we deal with very similar systems as shown from colloidal and microstructural characterization and no evidence can be found for the origin of the emergence of shear-thinning from these properties for the samples containing 1-hexadecanol and 1-octadecanol. A possible explanation is that for samples OD and HD at lower temperature, where the phenomenon is more evident and where the Brownian motion of particles is reduced, particles clustering is more favoured with respect to other samples due to interaction between the fatty alcohols and the SDS stabilizing layer. The disruption of the clusters under shearing could be the origin of the observed shear-thinning.

4. Conclusions

Concentrated colloidal dispersions in water of PMMA nano-capsules with sizes of less than 100 nm containing RT21HC, a commercial PCM with transition at 21 °C, with a concentration of 10 wt % with respect to the whole dispersion, have been successful prepared and characterized from the colloidal and thermophysical point of views. Different nucleating agents such 1-octadecanol,1-hexadecanol, methyl-stearate, methyl-palmitate and dodecanoic acid have been incorporated into the PMMA nano-capsules with the aim of reducing the phenomenon of supercooling and increase the apparent thermal capacity of the fluids. All the suspensions show good colloidal stability, moderate reductions of thermal diffusivity with respect to water, which is within the range 6–10 %, and moderate increase of dynamic viscosity, with Newtonian behaviour except for the samples containing fatty alcohols as nucleating agents that show a shear-thinning behaviour at 10 °C. It has been found that among the 5 nucleating agents incorporated into the nano-capsules, 1-octadecanol is the most effective in reducing solidification supercooling that is caused by nano-confinement, leading to a 5% increase of apparent thermal capacity with respect to reference sample not containing nucleating agents and an absolute increase of more than 10% with respect to pure water. This result demonstrates the potential of using these advanced colloidal systems as promising efficient fluids for thermal management and cooling applications.

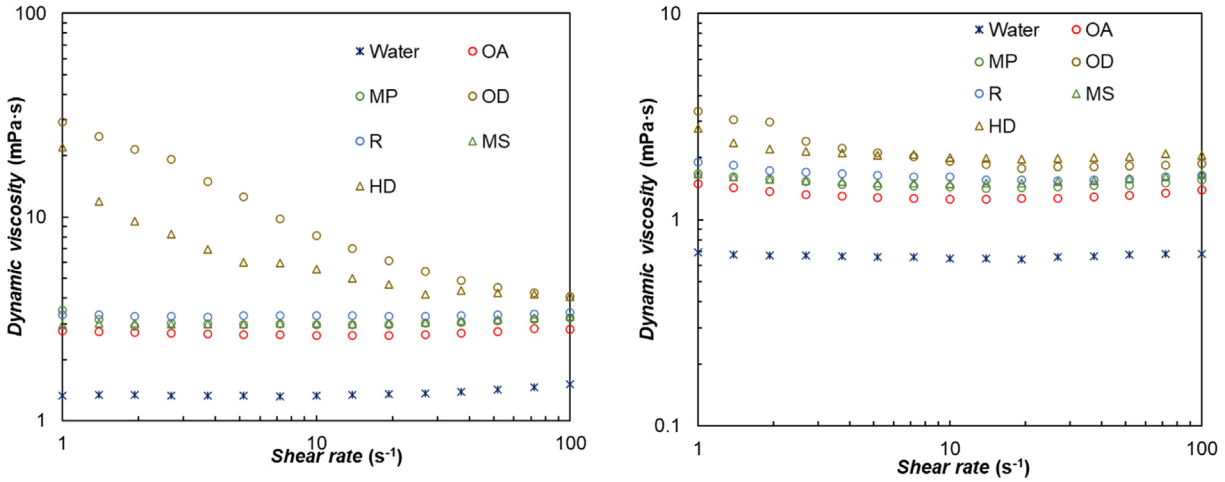

Fig. 7. Dynamic viscosity curves at 10 °C (left) and 40 °C (right).

CRediT authorship contribution statement

Filippo Agresti: Conceptualization, Validation, Investigation, Writing – original draft, Writing – review & editing. **David Cabaleiro:** Conceptualization, Validation, Investigation, Writing – review & editing. **Laura Fedele:** Validation, Investigation, Writing – review & editing. **Stefano Rossi:** Validation, Investigation, Writing – review & editing. **Simona Barison:** Conceptualization, Validation, Investigation, Writing – review & editing, Funding acquisition.

Data availability

Data will be made available on request.

Declaration of Competing Interest

The authors declare that they have no known competing financial interests or personal relationships that could have appeared to influence the work reported in this paper.

Acknowledgement

The authors would like to acknowledge the financial support of CNR through the project@CNR "Phase change material nanoemulsions for energy efficient cooling".

References

[1] A European Green Deal, https://ec.europa.eu/info/strategy/priorities-2019-2024/european-green-deal_en.
[2] T. Morimoto, M. Sugiyama, H. Kumano, Experimental study of heat transfer characteristics of phase change material emulsions in a horizontal circular tube, Appl. Therm. Eng. 188 (2021), https://doi.org/10.1016/J.APPLTHERMALENG.2021.116634.
[3] F. Wang, J. Cao, Z. Ling, Z. Zhang, X. Fang, Experimental and simulative investigations on a phase change material nano-emulsion-based liquid cooling thermal management system for a lithium-ion battery pack, Energy 207 (2020), https://doi.org/10.1016/J.ENERGY.2020.118215.
[4] S. Barison, D. Cabaleiro, S. Rossi, A. Kovtun, M. Melucci, F. Agresti, Paraffin–graphene oxide hybrid nano emulsions for thermal management systems, Colloids Surfaces A Physicochem. Eng. Asp. 627 (2021), https://doi.org/10.1016/J.COLSURFA.2021.127132.
[5] D. Cabaleiro, F. Agresti, S. Barison, M.A. Marcos, J.I. Prado, S. Rossi, S. Bobbo, L. Fedele, Development of paraffinic phase change material nanoemulsions for thermal energy storage and transport in low-temperature applications, Appl. Therm. Eng. 159 (2019), https://doi.org/10.1016/J.APPLTHERMALENG.2019.113868.
[6] D. Cabaleiro, S. Losada-Barreiro, F. Agresti, C. Hermida-Merino, L. Fedele, L. Lugo, S. Barison, M.M. Piñeiro, Development and Thermophysical Profile of Cetyl Alcohol-in-Water Nanoemulsions for Thermal Management, Fluids 7 (2022) 11, https://doi.org/10.3390/FLUIDS7010011.
[7] F. Agresti, L. Fedele, S. Rossi, D. Cabaleiro, S. Bobbo, G. Ischia, S. Barison, Nano-encapsulated PCM emulsions prepared by a solvent-assisted method for solar applications, Sol. Energy Mater. Sol. Cells. 194 (2019) 268–275, https://doi.org/10.1016/j.solmat.2019.02.021.
[8] E. Günther, L. Huang, H. Mehling, C. Dötsch, Subcooling in PCM emulsions - Part 2: Interpretation in terms of nucleation theory, Thermochim. Acta. 522 (2011) 199–204, https://doi.org/10.1016/j.tca.2011.04.027.
[9] K. Ghasemi, S. Tasnim, S. Mahmud, PCM, nano/microencapsulation and slurries: A review of fundamentals, categories, fabrication, numerical models and applications, Sustain. Energy Technol. Assessments. 52 (2022), https://doi.org/10.1016/J.SETA.2022.102084.
[10] A. Sari, C. Alkan, C. Bilgin, Micro/nano encapsulation of some paraffin eutectic mixtures with poly(methyl methacrylate) shell: Preparation, characterization and latent heat thermal energy storage properties, Appl. Energy. 136 (2014) 217–227, https://doi.org/10.1016/J.APENERGY.2014.09.047.
[11] Y. Yang, X. Ye, J. Luo, G. Song, Y. Liu, G. Tang, Polymethyl methacrylate based phase change microencapsulation for solar energy storage with silicon nitride, Sol. Energy. 115 (2015) 289–296, https://doi.org/10.1016/J.SOLENER.2015.02.036.
[12] A. Sari, C. Alkan, A. Biçer, A. Altuntaş, C. Bilgin, Micro/nanoencapsulated n-nonadecane with poly(methyl methacrylate) shell for thermal energy storage, Energy Convers. Manag. 86 (2014) 614–621, https://doi.org/10.1016/J.ENCONMAN.2014.05.092.
[13] J. Shi, X. Wu, R. Sun, B. Ban, J. Li, J. Chen, Nano-encapsulated phase change materials prepared by one-step interfacial polymerization for thermal energy storage, Mater. Chem. Phys. 231 (2019) 244–251, https://doi.org/10.1016/J.MATCHEMPHYS.2019.04.032.
[14] B. Maleki, A. Khadang, H. Maddah, M. Alizadeh, A. Kazemian, H.M. Ali, Development and thermal performance of nanoencapsulated PCM/ plaster wallboard for thermal energy storage in buildings, J. Build. Eng. 32 (2020), https://doi.org/10.1016/J.JOBE.2020.101727.
[15] H.Y. Woo, D.W. Lee, T.Y. Yoon, J.B. Kim, J.Y. Chae, T. Paik, Sub-100-nm Nearly Monodisperse n-Paraffin/PMMA Phase Change Nanobeads, Nanomater. 11 (2021) 204. https://doi.org/10.3390/NANO11010204.
[16] M. Rezvanpour, M. Hasanzadeh, D. Azizi, A. Rezvanpour, M. Alizadeh, Synthesis and characterization of micro-nanoencapsulated n-eicosane with PMMA shell as novel phase change materials for thermal energy storage, Mater. Chem. Phys. 215 (2018) 299–304, https://doi.org/10.1016/J.MATCHEMPHYS.2018.05.044.
[17] F. Agresti, A. Ferrario, S. Boldrini, A. Miozzo, F. Montagner, S. Barison, C. Pagura, M. Fabrizio, Temperature controlled photoacoustic device for thermal diffusivity measurements of liquids and nanofluids, Thermochim. Acta. 619 (2015) 48–52, https://doi.org/10.1016/j.tca.2015.09.017.
[18] X. Cheng, J.H. McCoy, J.N. Israelachvili, I. Cohen, Imaging the microscopic structure of shear thinning and thickening colloidal suspensions, Science 333 (2011) 1276–1279, https://doi.org/10.1126/science.1207032.
[19] X. Xu, S.A. Rice, A.R. Dinner, Relation between ordering and shear thinning in colloidal suspensions, Proc. Natl. Acad. Sci. 110 (2013) 3771–3776, https://doi.org/10.1073/PNAS.1301055110.
[20] L.B. Chen, B.J. Ackerson, C.F. Zukoski, Rheological consequences of microstructural transitions in colloidal crystals, J. Rheol. 38 (1994) 193, https://doi.org/10.1122/1.550498.
[21] R.L. Hoffman, Discontinuous and Dilatant Viscosity Behavior in Concentrated Suspensions. I. Observation of a Flow Instability, Trans. Soc. Rheol. 16 (1972) 155, https://doi.org/10.1122/1.549250.
[22] D. Gilbert, R. Valette, E. Lemaire, Impact of particle stiffness on shear-thinning of non-Brownian suspensions, J. Rheol. 66 (2022) 161, https://doi.org/10.1122/8.0000338.